Journal of Food Bioactives
International Society for Nutraceuticals and Functional Foods
Original Research
J. Food Bioact. 2020;9:79–87

Promoting effect of Se-allylselenocysteine on 7,12-dimethylbenz[a] anthracene (DMBA)/12-*O*-tetradecanoylphorbol-13-acetate (TPA)-induced skin tumorigenesis

An-Chin Cheng[a#], Wan-Ru Jiang[b#], Yu-Hsuan Hsiao[b], Vladimir Badmaev[c], Chi-Tang Ho[d], Roch-Chui Yu and Min-Hsiung Pan[b,e,f*]

[a]Department of Nutrition and Health Sciences, Chun Jung Christian University, Tainan, Taiwan
[b]Institute of Food Science and Technology, National Taiwan University, Taipei 10617, Taiwan
[c]American Medical Holdings Incorporated, New York, New York
[d]Department of Food Science, Rutgers University, New Brunswick, NJ 08901, USA
[e]Department of Medical Research, China Medical University Hospital, China Medical University, Taichung 40402, Taiwan
[f]Department of Health and Nutrition Biotechnology, Asia University, Taichung, Taiwan
[#]These authors contributed equally to this work.
[*]**Corresponding author:** Min-Hsiung Pan, Institute of Food Science and Technology, National Taiwan University, No. 1, Section 4, Roosevelt Road, Taipei 10617, Taiwan. Tel: +886 2 33664133; Fax: +886-2-33661771; E-mail: mhpan@ntu.edu.tw

DOI: 10.31665/JFB.2020.9221
Received: February 26, 2020; **Revised received & accepted:** March 31, 2020
Citation: Cheng, A.-C., Jiang, W.-R., Hsiao, Y.-H., Badmaev, V., Ho, C.-T., Yu, R.-C., and Pan, M.-H. (2020). Promoting effect of Se-allylselenocysteine on 7,12-dimethylbenz[a]anthracene (DMBA)/12-*O*-tetradecanoylphorbol-13-acetate (TPA)-induced skin tumorigenesis. J. Food Bioact. 9: 79–87.

Abstract

Se-allylselenocysteine (ASC), an analogue of garlic bioactive compound, has been shown to inhibit mammary carcinogenesis *in vivo* and cell growth *in vitro*. However, the function of ASC on anti-inflammatory effects remains largely unknown. Therefore, we investigated whether ASC has an anti-inflammatory effect on lipopolysaccharide (LPS)-induced inflammation or an anti-tumor effect promoting on DMBA/TPA-induced skin tumorigenesis and tried to elucidate the mechanisms involved. Herein, the results showed that ASC inhibited LPS-induced production of nitric oxide (NO) with a decreased protein level of inducible nitric oxide synthase (iNOS) in RAW 264.7 cells. However, ASC enhanced LPS-induced cyclooxygenase-2 (COX-2) protein levels and mRNA expression. Interestingly, we found for the first time that topical application of ASC on the dorsal skin of DMBA-initiated and TPA-promoted mice significantly accelerated skin tumorigenesis and raised tumor multiplicity as compared to the positive control group (DMBA/TPA). The number of tumours that were 1–3, 3–5, and >5 mm in size per mouse increased in a dose-dependent manner in the ASC pre-treated groups. Pre-treatment with ASC showed a significant increase in the expression of COX-2 compared with the positive control group. Thus, ASC may modulate the COX-2 protein expression and promote DMBA/TPA-induced skin cancer in mice.

Keywords: Anti-inflammation; Se-allylselenocysteine (ASC); Nitric oxide synthase (iNOS); Cyclooxygenase-2 (COX-2); 7,12-dimethylbenz [a]anthracene (DMBA)/12-*O*-tetradecanoylphorbol-13-acetate (TPA)-induced skin tumorigenesis.

1. Introduction

Production of NO and prostaglandins by iNOS and COX-2, respectively, are considered the most prominent molecular mechanisms during inflammatory responses (Florentino et al., 2017; Kim and Kang, 2016) and are also involved in multistage carcinogen-

esis, especially the promotion stage (Pan and Ho, 2008). Excessive and prolonged NO generation caused by the overexpression of iNOS has also been implicated in inflammation tumorigenesis, while COX-2-mediated prostaglandin production stimulates cell proliferation, invasion, and angiogenesis in cancer development (Qiu et al., 2017).

Garlic extract contains diverse array of organic polysulfide compounds such as diallyl sulfide (DAS), diallyl disulfide (DADS), and S-allylcysteine (SAC) which have potent anti-inflammation and anti-cancer properties. LPS activates NF-κB, a transcription factor that is involved in inflammatory response. Previous studies have indicated that aged red garlic extract and garlic oil derivatives such as DAS, DADS, and allyl methyl sulfide (AMS) could exert anti-inflammatory effects in LPS-stimulated RAW 264.7 macrophages through inhibition of iNOS expression, NO production, prostaglandin E_2 (PGE_2), and NF-κB (Liu et al., 2006; Shin et al., 2013; Lee et al., 2015; Ryu et al., 2015). ASC, an analogue of garlic compound, has been shown to exert an inhibitory effect on the growth of TM12 cells through modulating the expression of cell cycle regulatory proteins, inducing the loss of DNA integrity, and increasing the rate of apoptosis (Zhu et al., 2000a; Zhu et al., 2000b; Jiang et al., 2001). ASC was also found to inhibit mammary carcinogenesis *in vivo* and cell growth *in vitr*o (Ip et al., 1999). ASC did not induce the expression of cytochrome P450s (CYP) at a concentration of 100 μM. CYP, which is an important factor result in a risk at bioactivation of pro-carcinogens. ASC also elevates glutathione-*S*-transferase (GST) mRNA level, the induction of GST normally enhances the detoxification ability (AC't Hoen et al., 2002). Our previous study found that ASC could induce autophagy and epigenetic regulation of protocadherin 17 (PCDH17) in human colorectal adenocarcinoma cells (Wu et al., 2015). However, the function of ASC on anti-inflammatory effects remains unknown.

The two-stage skin carcinogenesis model is a well-characterized model of multistep carcinogenesis. A single dose of 7,12-dimethylbenz[a]anthracene (DMBA) was applied on mouse skin to mutate the *Ha-ras* gene at codon 61 (A to T) (Nelson et al., 1992), which resulted in the transformation of the original normal cells to cancer cells (Shen et al., 2014). Repeated treatment with TPA could support the growth of transformed cells by activating inflammation-related cytokines (Chun et al., 2004; Passos et al., 2013), such as epidermal growth factor receptor (EGFR) (Casanova et al., 2002) and extracellular signal-regulated kinase (ERK) (Bourcier et al., 2006).The development of skin tumors in female ICR mice in response to treatment with DMBA and phorobol 12-myristate 13-acetate (TPA) can explain the multistep process of carcinogenesis including initiation, promotion, and progression (Balmain et al., 1984; Arora et al., 2013; Ma et al., 2013).

In this study, we examined the effects of ASC on LPS-induced inflammatory responses of RAW 264.7 murine macrophages. The association between the suppression of NF-κB and the inhibition of NO production was also assessed. We also investigated its anticancer potential against DMBA and TPA-induced skin cancer. The results indicated that ASC suppressed the production of NF-κB, thereby inhibiting the expression of iNOS in activated macrophages. However, this study evidenced that ASC had tumor induction effects on a DMBA/TPA skin carcinogenesis protocol. Data showed that ASC could significantly accelerate mouse skin tumorigenesis and raise tumor multiplicity more than the positive control group. However, future investigations are warranted to determine the mechanisms of tumorigenesis effects of ASC on DMBA/TPA induced skin cancer.

2. Materials and methods

2.1. Materials

Lipopolysaccharide (LPS) (Escherichia coli 0127:E8), Phorobol 12-myristate 13-acetate (TPA), and 7,12-dimethylbenz[a]anthracene (DMBA) were purchased from Sigma Chemical (St. Louis, MO). Se-allylselenocysteine was provided by American Medical Holding, Inc. (New York, NY, USA). Reverse transcription polymerase chain reaction (RT-PCR) reagents were purchased from TaKaRa (Mountain View, CA, USA).

2.2. Animals

Female Institute of Cancer Research mice at 5–6 weeks age were obtained from the BioLASCO Experimental Animal Center (BioLASCO Taiwan Co., Ltd, Taipei, Taiwan). All animals were housed in a controlled atmosphere (25 ± 1 °C at 50% relative humidity) and with a 12 hr light-12 hr dark cycle. All experimental protocols used in these animal experiments were approved by the Institutional Animal Care and Use Committee (IACUC B201700174) of National Taiwan University.

The dorsal skin of each mouse was shaved with surgical clippers before the application of the tested compound. ASC and TPA were dissolved in 200 μL of acetone and applied topically to the shaved area of each mouse.

2.3. Cell culture

RAW 264.7 murine macrophage cells obtained from the American Type Culture Collection (Rockville, MD, USA) were cultured in Dulbecco's Modified Eagle Medium (DMEM), supplemented with 10% endotoxin-free, heat-inactivated fetal bovine serum, 10,000 units/mL penicillin, and 10,000 μg/mL streptomycin (GIBCO, Grand Island, NY, USA) and kept at 37 °C in a humidified atmosphere with 5% CO_2 in air, according to ATCC recommendations. When the cells reached a density of 2–3 × 10^6 cells/mL, they were activated by incubation in medium containing LPS (100 ng/mL). Various concentrations of test compounds dissolved in ddH_2O were added to the LPS.

2.4. Cell viability assay

The RAW 264.7 cells were cultivated at a density of 1 × 10^6 cells in a 24-well plate. The ASC studied was added to the medium 12 hr after inoculation. The cells were harvested after 24 hr. Viability was determined by trypan blue.

2.5. Nitrite assay

The nitrite concentration in the culture medium was measured as an indicator of NO production, according to the Griess reaction. The cells were treated with LPS (100 ng/mL) for 24 h in the presence of ASC or vehicle solution. The conditional medium (100 μL) was taken and mixed with an equal volume of the Griess reagent (1% sulfanilamide in 5% phosphoric acid and 0.1% naphthylethylenediamine dihydrochloride in water). Nitrite production was determined by reading the absorbance at 550 nm. A standard curve was generated with $NaNO_2$.

2.6. Total protein extraction

Total protein extracts (for iNOS, COX-2, β-actin, p-IκBα, and IκBα) were prepared in a gold lysis buffer (10% Glycerol, 1% Triton X-100, 137 mM NaCl, 10 mM NaF, 5 mM ethylenediaminetetraacetic acid (EDTA), 1 mM ethylenebis(oxyethylenenitrilo)tetraacetic acid (EGTA), 20 mM Tris pH 7.9, 1 mM Na_3VO_4, 100 mM-glycerol phosphate, and 1 mM sodium pyrophosphate) for 30 min at 4 °C. The supernatants containing total proteins were obtained by centrifugation at 10,000 × g for 30 min and stored at −20 °C until tested.

2.7. Western blotting

Whole protein extracts were obtained by homogenizing skin samples and cells, flash-frozen in liquid nitrogen, in a whole cell lysis buffer. Proteins from (50 μg) whole-cell lysates were resolved by 10% SDS-PAGE, transferred onto polyvinylidene difluoride membranes (Immobilon P, Millipore, Bedford, MA, USA), and then probed with a primary antibody followed by a secondary antibody conjugated with horseradish peroxidase. The immunocomplexes were visualized with Western Chemiluminescent HRP Substrate (ECL) (Millipore, Amersham, UK).

2.8. Reverse transcription-polymerase chain reaction (RT-PCR)

The level of COX-2 mRNA expression was measured by RT-PCR. Total RNA was isolated using TRIzol reagent (Sigma-Aldrich, St. Louis, MO, USA) as recommended by the manufacturer's instructions. Briefly, total RNA (1 μg) was performed by PCR in a final volume of 50 μL containing 25 L 2 × 1 step buffer, 2 L PrimeScript 1 step enzyme mix, 1 L upstream primer (20 mer), 1 L downstream reverse primer (20 mer), and RNase free dH_2O. The specific PCR primers used in this experiment are listed as follow. COX-2: primer sequence, sense: 5′-GGAGAGACTATCAAGATAGTGATC-3′, antisense: 5′-ATGGTCAGTAGACTTTTACAGCTC-3′; β-actin, sense: 5′-AAGAGAGGCATCCTCACCCT-3′, antisense: 5′-TACATGGCTGGGGTGTTGAA-3′.

The PCR conditions were as follows. After an initial denaturation for 2 min at 94 °C, 30 cycles of amplification (denaturation at 94 °C for 30 s, primer annealing at 50 °C for 30 s and extension at 72 °C for 1 min) were performed and samples were kept at 4 °C following PCR. A 15 μL sample of each PCR product was electrophoresed on a 2% agarose gel and visualized by ethidium bromide staining. Each value was normalized to the expression of β-actin. The values presented are the mean ± SE of at least triplicate measurements.

2.9. Transient transfection and luciferase assay

NF-κB luciferase-stable RAW 264.7 cells were seeded and cultivated at a density of 1 × 106 cells in a 24-well plate. After 12 h, the cells were co-incubated with 100 ng/mL LPS with or without ASC for an additional 24 h. The cells were collected into an Eppendorf tube, centrifuged (1,000 × g, 4 °C, 10 min) and then we removed the supernatant. Luciferase activity was assayed by means of the reporter gene assay system (Perkin Elmer, Waltham, MA, USA), with 100 μL of cell lysate used in each assay.

2.10. Two-stage tumorigenesis in mouse skin

The anti-tumor promoting activity of ASC was examined by a standard initiation-promotion with DMBA and TPA, as reported previously (DiGiovanni, 1992). One group was composed of 12 female ICR mice. These mice were given commercial rodent pellets and fresh tap water ad libitum, both of which were changed twice a week. The dorsal region of each mouse was shaved with an electric clipper 2 days before initiation. Mice at 6 weeks old were started on 200 nmol DMBA in 200 μL acetone; control mice received 200 μL acetone only. One week after initiation, the mice were treated topically with 200 μL acetone or promoted with TPA (5 nmol in 200 μL acetone) twice a week for 20 weeks. In the other two groups, the mice were treated with ASC (1 and 5 mol in 200 μL acetone) 30 min before each TPA treatment. Tumors of at least 1 mm in diameter were counted and recorded every week. The results were expressed as the average number of tumors per mouse, percentage of tumor-bearing mice, and average tumor weight per mouse.

2.11. Statistical analysis

Quantitative data represent mean values with the respective standard error of the mean (SE) corresponding to three or more replicates. A One-Way Student's t-test was used to assess the statistical significance between the LPS and ASC plus LPS-treated cells. Data were considered statistically significant at $p < 0.05$.

3. Results

3.1. ASC suppresses LPS-induced NO production in RAW 264.7 macrophages

We first tested the effect of ASC on cell viability to exam the cytotoxic effects of ASC on RAW 264.7 macrophages. RAW 264.7 macrophages were treated with different concentrations of ASC as indicated. After 24 hr of treatment, the viability of cells was determined by trypan blue exclusion assay. As shown in Figure 1, ASC did not show cytotoxic effects on RAW 264.7 macrophages at 5–50 μM of treatment. To evaluate the inhibitory effects of ASC on LPS-stimulated NO production in RAW 264.7 cells, the cells were treated with LPS (100 ng/mL) only or with different concentrations of ASC for 24 hr. At the end of incubation time, 100 μL of the culture medium was collected for nitrite assay. As shown in Figure 2, the nitrite in LPS-stimulated cells is about 10 times the concentration of the negative control group, and the LPS-induced nitrite production was reduced significantly in 50 μM of ASC treated RAW 264.7 macrophages.

3.2. Effects of ASC on the LPS-induced expressions of iNOS and Cox-2 proteins and mRNA

In unstimulated RAW 264.7 cells, iNOS and COX-2 proteins were undetectable. Following stimulation with LPS, elevated levels of iNOS and COX-2 proteins were detected in RAW 264.7 cells. According to previous data, nitrite production was reduced significantly in RAW 264.7 cells treated with 50 μM of ASC. Likewise, iNOS expression was inhibited markedly by ASC at 50 μM in a similar manner (Fig. 3). These results indicate that the reduced expressions of iNOS by ASC were responsible for the inhibition of LPS-induced NO production. However, ASC could significantly enhance the levels of COX-2 protein (Fig. 3). To detect the effects of ASC on LPS-induced COX-2 mRNA expression by RT-PCR,

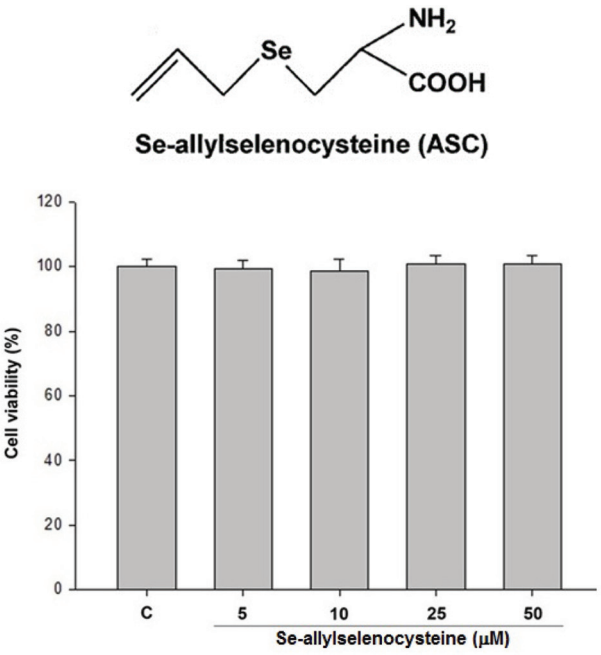

Figure 1. Effects of ASC on cell viability. RAW 264.7 cells were treated with 5, 10, 25, 50 μM of ASC for 24 hr. The viability of cells was determined by trypan blue assay. The values are expressed as means S.E. of triplicate tests. **P* < 0.05, ***P* < 0.01, ****P* < 0.001.

analysis showed that the expression of COX-2 mRNA was correlated with the levels of COX-2 protein (Fig. 4).

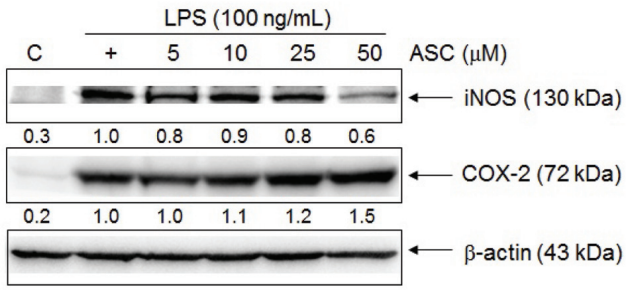

Figure 3. Effects of ASC on LPS-induced iNOS and COX-2 protein level in RAW 264.7 cells. The cells were treated with different concentrations of ASC and LPS (100 ng/mL) for 24 hr. An equal amount of total proteins (50 μg) were subjected to 8% SDS-PAGE. The expression of iNOS, COX-2 and β-actin was detected by western blot using specific antibodies. These experiments were repeated three times with similar results. Relative protein levels were quantified using Image J.

3.3. Effects of ASC on the LPS-induced IκB phosphorylations and NF-κB activation

In this study, we investigated whether ASC inhibited the LPS-stimulated degradation of IκB in RAW 264.7 macrophages by Western blotting. Figure 5a shows that LPS-induced IκB-α degradation was significantly blocked by ASC. Transient transfection with pNF-κB-Luc reporter plasmid was applied to confirm whether ASC inhibited NF-κB activity in LPS-activated macrophages. As shown in Figure 5b, LPS-induced NF-κB activity was elevated fivefold in these transfected cells, but the effects were reduced by ASC treatment in a dose-dependent manner.

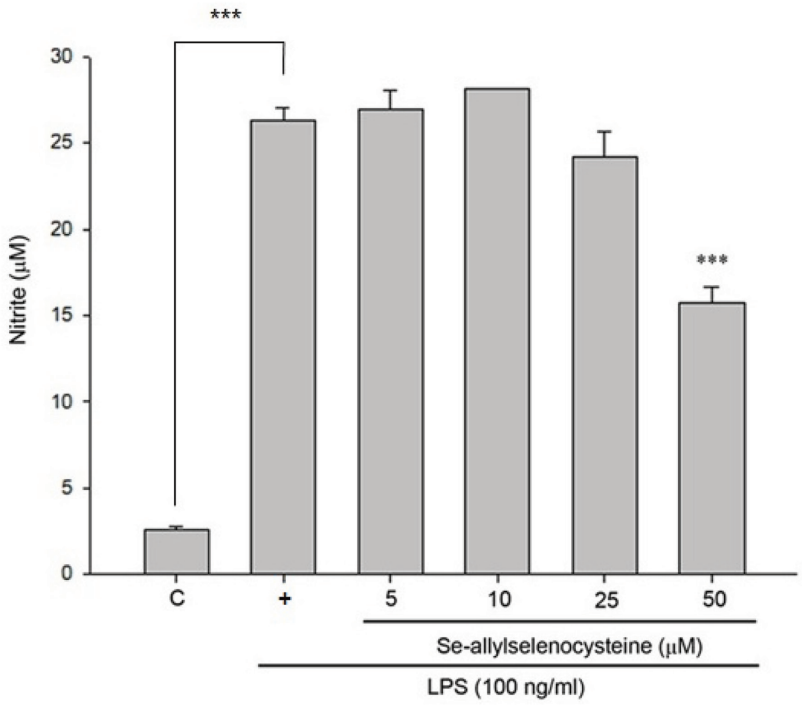

Figure 2. Inhibitory effects of ASC on NO production in LPS-stimulated RAW 264.7 cells. The cells were treated with LPS (100 ng/mL) only or with different concentrations of ASC for 24 hr. At the end of incubation time, 100 μL of the culture medium was collected for nitrite assay. The values are expressed as means S.E. of triplicate tests. **P* < 0.05, ***P* < 0.01, ****P* < 0.001 (control versus LPS alone; LPS alone versus ASC 5, 10, 25 and 50 μM).

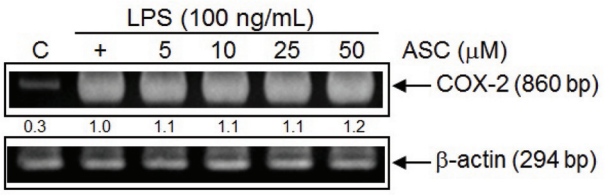

Figure 4. RT-PCR analysis of the effects of ASC on LPS-induced COX-2 mRNA expression. Cells were treated with LPS (100 ng/mL) and ASC (5, 10, 25, 50 μM) for 6 hr, and total RNA was subjected to RT-PCR with the primers COX-2 with β-actin as internal control. The PCR product was resolved in 2% agarose gel. These experiments were repeated three times with similar results. Quantification of COX-2 expression was normalized to β-actin using Image J.

3.4. Tumour-promoting effect of ASC on DMBA/TPA-induced mouse skin tumorigenesis

For testing the effect of ASC on DMBA/TPA-induced mouse skin tumourigenesis, we examined the body weight of the mice for 20 weeks and found no difference in weight between the ASC treated mice and those without treatment (Fig. 6a). Subsequently, tumours were analyzed histologically. As shown in Figure 6b and c, ASC significantly accelerated the frequency and progression of chemically-induced papillomas of the skin and raised an average number of tumours in the mice. 7 weeks after the ASC administration, the first skin tumours (≥1 mm diameter) occurred in mice treated with 1 μmol/200 μL and 5 μmol/200 μL. Over the subsequent 11 weeks of tumour promotion, the number of tumours per mouse increased much faster in ASC 1 μmol /200 μL treated and the positive control mice. Moreover, 100% of the ASC 5 μmol/200 μL treated mice had developed numerous tumours at week 9.

Counting of tumours with an area of ≥1 mm^2 revealed that ASC 1 μmol/200 μL treated mice developed on average 31 and ASC 5 μmol/200 μL treated mice displayed 35 papillomas of this size, both of which were higher than the positive control. The number of tumours that were 1–3, 3–5, 5–7, and >7 mm in size per mouse increased in a dose-dependent manner in the ASC pre-treated groups (Fig. 6d). Tumour weight was also increased in ASC pre-treated groups (Fig. 6e). As shown in Figure 6f, characteristic squamous pearls were clearly observed on the uncovered dorsal skin of mice with topical applications of DMBA/TPA. ASC mice combined could induce more papillomas per mouse in total and larger size tumours per mouse than the positive control group in a dose-dependent manner.

3.5. Pro-inflammation effect of ASC on DMBA/TPA-induced mouse skin tumorigenesis

COX-2 is often undetectable in normal tissue, whereas its expression is observably higher in tumour tissue (Cao and Prescott, 2002). The pro-inflammatory activity of ASC can be demonstrated by its effect on COX-2 expression in TPA-induced mouse skin. The results showed that topical application of TPA to mouse dorsal skin could upregulate the expression of COX-2 compared to the acetone treated control group, whereas pre-treatment with ASC caused a marked increase in COX-2 expression in a dose-dependent manner compared to the DMBA/TPA control. (Fig. 7).

4. Discussion

First, we tested the effect of ASC on cell viability to exclude the possibility that the decreased nitrite production in ASC-treated cells was due to growth inhibition. As shown in Figure 1, ASC did not show cytotoxic effects on RAW 264.7 macrophages at 5–50 μM treatment. According to Figure 2, nitrite production was reduced significantly in RAW 264.7 cells treated with 50 μM of ASC. We next tested the level of iNOS expression, in unstimulated RAW 264.7 cells, iNOS proteins were undetectable. Following stimulation with LPS, elevated levels of iNOS proteins were detected in RAW 264.7 cells. As shown in Figure 3, iNOS expression was also markedly inhibited by ASC at 50 μM. These results indicate that ASC could decrease inflammation by inhibiting LPS-induced iNOS expression and NO production.

NF-κB is a key regulator of the various genes involved in inflammatory responses (Xie et al., 1994). In unstimulated cells, NF-κB is sequestered in the cytoplasm by its inhibitor, IκB. Under LPS

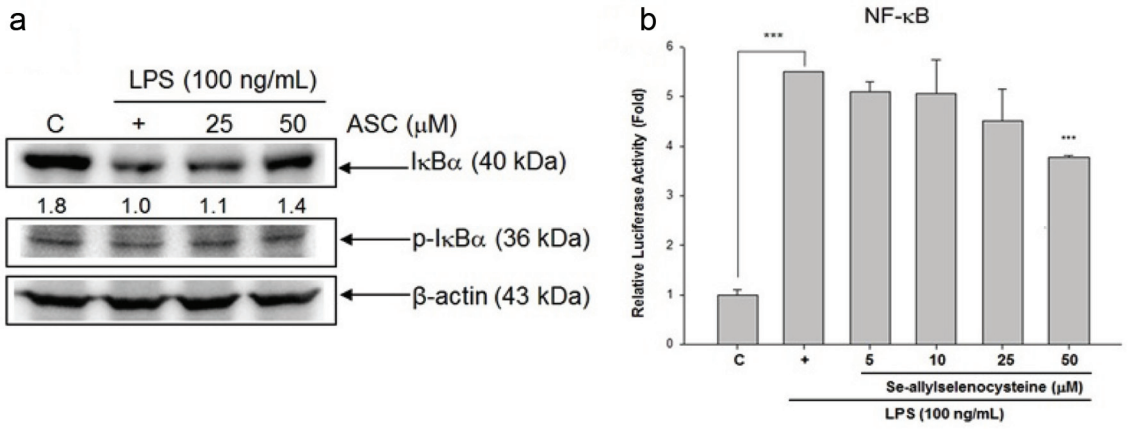

Figure 5. Effects of ASC on LPS-induced phosphorylation and degradation of IκB and NF-κB-luciferase (luc) activation. (a) RAW 264.7 cells were treated with LPS (100 ng/mL) and ASC, and total cellular lysates were prepared and analysed for the content of IκBα, p-IκBα, and β-actin by western blot. Quantification of IκB and p-IκBα protein level were normalized to β-actin using Image J. (b) The cells were treated with LPS (100 ng/mL) with or without ASC for 24 hr. Then, cells were collected for measuring luciferase activity assay. *P < 0.05, **P < 0.01, ***P < 0.001 (control versus LPS alone; LPS alone versus ASC 5, 10, 25, and 50 μM)

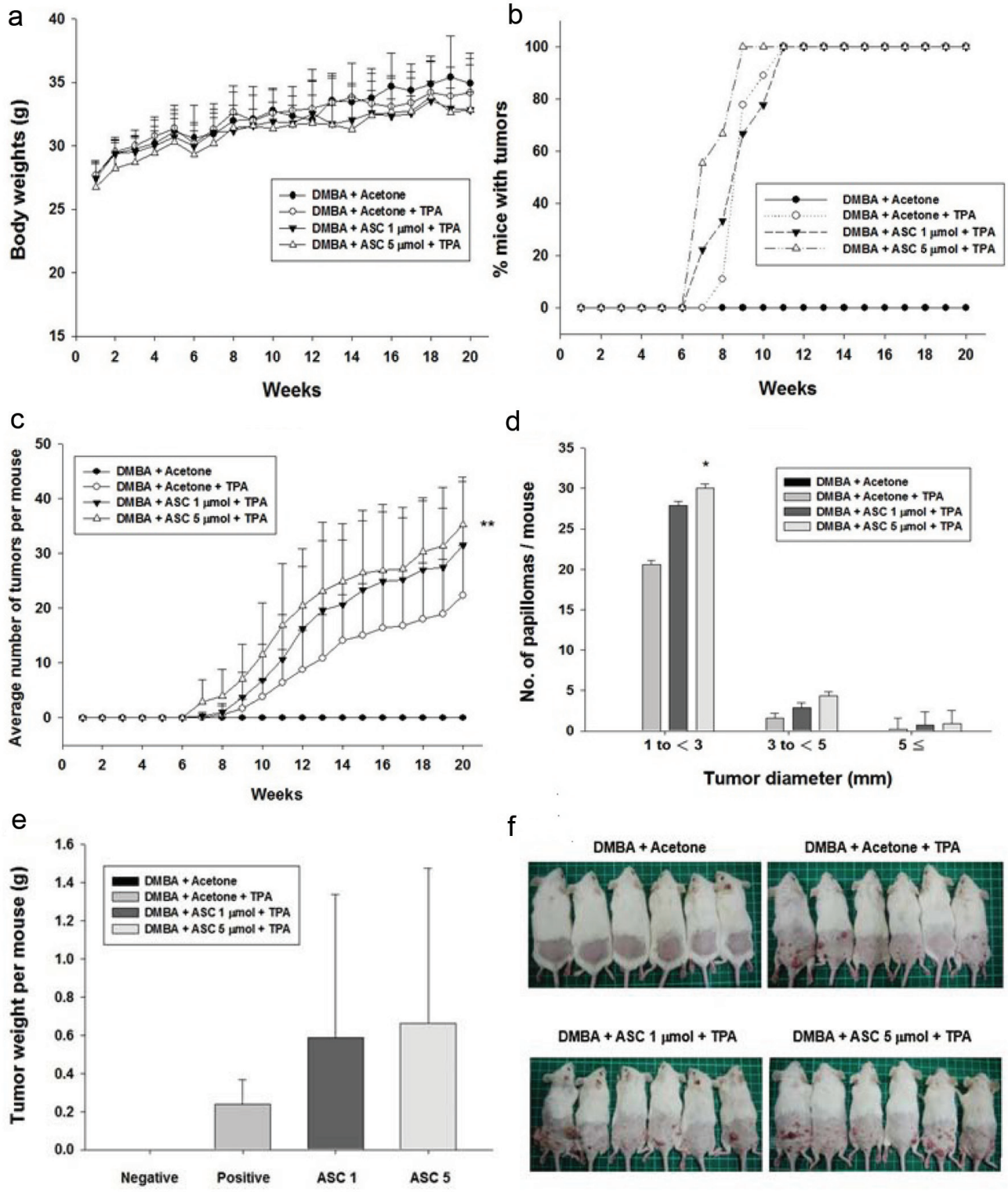

Figure 6. The promoting effect of ASC on DMBA/TPA-induced skin tumorigenesis in ICR mice. Female ICR mice received vehicle (acetone) or ASC (1 or 5 μmol) 30 min prior to each topical application of TPA (5 nmol) twice weekly for 20 weeks following DMBA-initiation, as described in materials and methods. Control animals received vehicle alone and did not produced papillomas. (a) The body weight of mice during skin tumour promotion. (b) Average number of tumours per mouse (tumour multiplicity). (c) Percentage of mice with papillomas (tumour incidence). (d) Size distribution of papillomas. (e) Tumour weight per mouse on control groups and ASC-treated mice. (f) Representative photographs of each group are shown at the end of week 20. *Significantly different from the corresponding TPA value at *P<0.05, **P<0.01, and ***P<0.001.

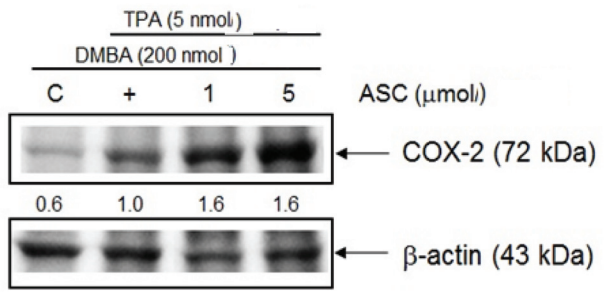

Figure 7. ASC up-regulate COX-2 protein level on DMBA/TPA-induced skin tumorigenesis. Shaven backs of female ICR mice were treated with ASC (1 or 5 μmol) 30 min prior to TPA (5 nmol) twice weekly for 20 weeks following DMBA-initiation, and control animals were treated with acetone only for 20 weeks following DMBA-initiation. Mice were sacrificed after 20 weeks and skin fractions were prepared from the skin/tumours of each group. The protein expression was determined by western blot analysis as described in the text. Quantification of COX-2 protein levels were normalized to β-actin using Image J. The data is representative of three different sets of animals giving a similar trend.

stimulation, IκB is phosphorylated and degraded by IκB kinase, ubiquitinated, and rapidly breaks away from NF-κB. NF-κB then translocate to the nucleus, where it binds to DNA and activates the transcription of iNOS and COX-2 (Rice and Ernst, 1993). As shown in Figure 5a and b, the LPS-induced IκB-α degradation was significantly blocked by ASC, and LPS-induced NF-κB activity was reduced by ASC treatment in a dose-dependent manner. The above findings show that ASC suppressed iNOS expression at least in part via the NF-κB-dependent mechanism.

COX-2 is a rate-limiting enzyme produced during the production of prostaglandins, and prostaglandins play an important role in inflammation and tumour progression (Seibert and Masferrer, 1994; Wang et al., 2007). COX-2 is often undetectable in normal tissue, whereas its expression is observably higher in many epithelial cancers (Cao and Prescott, 2002; Wang and Dubois, 2006). Epidemiological and clinical study has shown as higher as COX-2 is expressed, a poorer of prognosis is associated (Sobolewski et al., 2010). These reports showed that COX-2 has a multi-step role in tumorigenesis, whether in tumour promotion at early stage or at late development of chemoresistance and metastatic formation (Sarkar et al., 2007). According to Figure 3, ASC significantly enhanced the levels of COX-2 protein. RT-PCR analysis of the effects of ASC on LPS-induced COX-2 mRNA expression showed that pre-treatment with ASC caused a marked increase in COX-2 mRNA expression in a dose-dependent manner (Fig. 4). These results demonstrated that the COX-2-promoting effect of ASC was responsible for the pro-inflammatory effects in LPS-stimulated RAW 264.7 cells.

Selenium is one of the essential minerals for life but it detected to be toxic at low concentration and has been studied many years (Arnault and Auger, 2006). On the other hand, evidence showed that selenium could alter the metabolism of carcinogens in liver by played role in the mixed function oxidase system (Steinmetz and Potter, 1996). There are many studies demonstrating that ASC exhibits anti-carcinogenesis effects in vivo and in vitro (Zhu et al., 2000a; Zhu et al., 2000b; Jiang et al., 2001). In order to study the effect of ASC on the tumourigenesis, we employed a well-established two-stage model of chemical skin carcinogenesis in female ICR mice based on DMBA/TPA treatments (DiGiovanni, 1992) as papilloma formation can be induced by the two-stage carcinogenesis protocol (Kemp, 2005). Throughout the experiment, there was no noticeable difference in weight between the ASC-treated mice and those without treatment (Fig. 6a). In our previous study, ASC showed an anti-proliferative activity in colorectal cancer cell lines including HT-29 and COLO 205 cells at the concentration of ASC in 75 and 100 μM (Wu et al., 2015). These results indicated that the topical application of ASC did not result in systemic toxicity under a range of dosage condition. However, high dosage of Se could cause toxicity in plants. In general, the content of Se in plant tissues caused toxicity is around 5 mg kg^{-1} dry weight. The Se tolerance range in crop plants are quietly different, for instance, in rice 2 mg kg^{-1} dry weight is the maximum levels of Se, in wheat is 4.9 mg kg^{-1} dry weight, while Dutch clover can tolerant 330 mg kg^{-1} dry weight (Kolbert et al., 2018). Based on these results, we suggested that a relatively higher dosage of Se-compounds may cause cell toxicity and induce inflammation by increasing COX-2 expression. On the other hand, topical application of ASC on the dorsal skin of DMBA-initiated and TPA-promoted mice did not suppress but significantly accelerated skin tumorigenesis and raised tumor multiplicity (Fig. 6b, c, d). Because our study is based on the model of applying the drug to mouse skin, it is a reasonable inference that ASC needs to metabolize to other derivatives in vivo to exert its inhibitory effect on cancer.

Capsaicin, a pungent ingredient of chili peppers, has widely reported anticancer activities (Lin et al., 2016; Qian et al., 2016) and was suggested to have a clinical significance in tumor therapy (Dasgupta et al., 1998; Sharma et al., 2013). However, topical application of capsaicin on the dorsal skin of DMBA/TPA-induced skin tumorigenesis could significantly promote tumor formation and induce more numerous and larger skin tumors by modulating inflammation (Liu et al., 2015). The similarity between our findings and Liu's report suggests that the tumour promoting effects by ASC may occur via inflammation regulating (Liu et al., 2015). Previous studies have indicated COX-2 overproduction following DMBA/TPA treatment in a variety of cell types, leading to the suggestion that COX-2 production in microenvironment cells modulates tumor progression (Müller-Decker et al., 2002). Jiao et al. (2014) also indicated that COX-2 elevation in DMBA/TPA-treated epithelial cells is required for DMBA/TPA-driven papilloma appearance and progression. The effect of ASC on DMBA/TPA-induced mouse skin tumourigenesis showed that pre-treatment with ASC causes a marked increase in COX-2 expression in a dose-dependent manner compared to the DMBA/TPA control (Fig. 7). These results demonstrated that the COX-2-promoting effect of ASC was responsible for the pro-inflammatory and papilloma progression activity in DMBA/TPA induced mouse skin.

Several studies have indicated that angiogenic activators play an important part in the growth and spread of tumors. Disturbance of the balance between endogenous activators such as vascular endothelial growth factor (VEGF) and inhibitors of angiogenesis in the tumor microenvironment strongly induce tumor angiogenesis (Yamamizu et al., 2015). Angiogenesis is a normal and vital process in growth and development as well as in wound healing. Previous study substantiated that aged garlic extract exerts beneficial effects on wound healing (Ejaz et al., 2009), and garlic likely prevents the formation of peritoneal adhesions in a rat model (Sahbaz et al., 2014). Therefore, we presume that the tumor-promoting effect of ASC on DMBA-initiated and TPA-promoted skin tumorigenesis may be in part due to its effects on wound healing via angiogenesis.

In summary, the present results speculate that ASC may modulate inflammatory processes via different signal-generating pathways in complex microenvironments. COX-2 plays a crucial role in the tumour-promoting and papilloma progression effects of ASC on DMBA/TPA-induced skin cancer in mice. However, future investigations need to clarify the underlying molecular mechanisms

of cancer-promoting effects of ASC on DMBA-induced skin carcinogenesis in mice.

Acknowledgments

This study was supported by the Ministry of Science and Technology [108-2023-B-002-016-MY3 and 108-2321-B-002 -020].

Data availability

The data that support the findings of this study are available from the corresponding author upon reasonable request.

Conflict of interest

All authors declare that there are no conflicts of interest.

References

AC't Hoen, P., Rooseboom, M., Bijsterbosch, M.K., van Berkel, T.J., Vermeulen, N.P., and Commandeur, J.N. (2002). Induction of glutathione-S-transferase mRNA levels by chemopreventive selenocysteine Se-conjugates. Biochem. Pharmacol. 63(10): 1843–1849.

Arnault, I., and Auger, J. (2006). Seleno-compounds in garlic and onion. J. Chromatogr. A 1112(1-2): 23–30.

Arora, N., Bansal, M.P., and Koul, A. (2013). Modulatory effects of Azadirachta indica leaf extract on cutaneous and hepatic biochemical status during promotion phase of DMBA/TPA-induced skin tumorigenesis in mice. Indian J. Biochem. Biophys. 50: 105–113.

Balmain, A., Ramsden, M., Bowden, G.T., and Smith, J. (1984). Activation of the mouse cellular Harvey-ras gene in chemically induced benign skin papillomas. Nature 307(5952): 658–660.

Bourcier, C., Jacquel, A., Hess, J., Peyrottes, I., Angel, P., Hofman, P., Auberger, P., Pouyssegur, J., and Pages, G. (2006). p44 mitogen-activated protein kinase (extracellular signal-regulated kinase 1)-dependent signaling contributes to epithelial skin carcinogenesis. Cancer Res. 66(5): 2700–2707.

Cao, Y., and Prescott, S.M. (2002). Many actions of cyclooxygenase-2 in cellular dynamics and in cancer. J. Cell Physiol. 190(3): 279–286.

Casanova, M.L., Larcher, F., Casanova, B., Murillas, R., Fernandez-Acenero, M.J., Villanueva, C., Martinez-Palacio, J., Ullrich, A., Conti, C.J., and Jorcano, J.L. (2002). A critical role for ras-mediated, epidermal growth factor receptor-dependent angiogenesis in mouse skin carcinogenesis. Cancer Res. 62(12): 3402–3407.

Chun, K.S., Kim, S.H., Song, Y.S., and Surh, Y.J. (2004). Celecoxib inhibits phorbol ester-induced expression of COX-2 and activation of AP-1 and p38 MAP kinase in mouse skin. Carcinogenesis 25(5): 713–722.

Dasgupta, P., Chandiramani, V., Parkinson, M.C., Beckett, A., and Fowler, C.J. (1998). Treating the human bladder with capsaicin: is it safe? Eur. Urol. 33(1): 28–31.

DiGiovanni, J. (1992). Multistage carcinogenesis in mouse skin. Pharmacol. Ther. 54(1): 63–128.

Ejaz, S., Chekarova, I., Cho, J.W., Lee, S.Y., Ashraf, S., and Lim, C.W. (2009). Effect of aged garlic extract on wound healing: a new frontier in wound management. Drug Chem. Toxicol. 32(3): 191–203.

Florentino, I.F., Silva, D.P., Silva, D.M., Cardoso, C.S., Moreira, A.L., Borges, C.L., Soares, C.M.A., Galdino, P.M., Lião, L.M., Ghedini, P.C., Menegatti, R., and Costa, E.A. (2017). Potential anti-inflammatory effect of LQFM-021 in carrageenan-induced inflammation: the role of nitric oxide. Nitric Oxide. 69: 35–44.

Ip, C., Zhu, Z., Thompson, H.J., Lisk, D., and Ganther, H.E. (1999). Chemoprevention of mammary cancer with Se-allylselenocysteine and other selenoamino acids in the rat. Anticancer Res. 19(4B): 2875–2880.

Jiang, W., Zhu, Z., Ganther, H.E., Ip, C., and Thompson, H.J. (2001). Molecular mechanisms associated with Se-allylselenocysteine regulation of cell proliferation and apoptosis. Cancer Lett. 162(2): 167–173.

Jiao, J., Ishikawa, T.O., Dumlao, D.S., Norris, P.C., Magyar, C.E., Mikulec, C., Catapang, A., Dennis, E.A., Fischer, S.M., and Herschman, H.R. (2014). Targeted deletion and lipidomic analysis identify epithelial cell COX-2 as a major driver of chemically induced skin cancer. Mol. Cancer Res. 12(11): 1677–1688.

Kemp, C.J. (2005). Multistep skin cancer in mice as a model to study the evolution of cancer cells. Semin. Cancer Biol. 15(6): 460–473.

Kim, K.Y., and Kang, H. (2016). Sakuranetin Inhibits Inflammatory Enzyme, Cytokine, and Costimulatory Molecule Expression in Macrophages through Modulation of JNK, p38, and STAT1. J. Evidence-Based Complementary Altern. Med. 2016: 9824203.

Kolbert, Z., Molnár, Á., Feigl, G., and van Hoewyk, D. (2018). Plant selenium toxicity: Proteome in the crosshairs. J. Plant Physiol. 232: 291–300.

Lee, H.H., Han, M.H., Hwang, H.J., Kim, G.Y., Moon, S.K., Hyun, J.W., Kim, W.J., and Choi, Y.H. (2015). Diallyl trisulfide exerts anti-inflammatory effects in lipopolysaccharide-stimulated RAW 264.7 macrophages by suppressing the Toll-like receptor 4/nuclear factor-kappa B pathway. Int. J. Mol. Med. 35(2): 487–495.

Lin, M.H., Lee, Y.H., Cheng, H.L., Chen, H.Y., Jhuang, F.H., and Chueh, P.J. (2016). Capsaicin Inhibits Multiple Bladder Cancer Cell Phenotypes by Inhibiting Tumor-Associated NADH Oxidase (tNOX) and Sirtuin1 (SIRT1). Molecules 21(7): 849.

Liu, K.L., Chen, H.W., Wang, R.Y., Lei, Y.P., Sheen, L.Y., and Lii, C.K. (2006). DATS reduces LPS-induced iNOS expression, NO production, oxidative stress, and NF-kappaB activation in RAW 264.7 macrophages. J. Agric. Food Chem. 54(9): 3472–3478.

Liu, Z., Zhu, P., Tao, Y., Shen, C., Wang, S., Zhao, L., Wu, H., Fan, F., Lin, C., Chen, C., Zhu, Z., Wei, Z., Sun, L., Liu, Y., Wang, A., and Lu, Y. (2015). Cancer-promoting effect of capsaicin on DMBA/TPA-induced skin tumorigenesis by modulating inflammation, Erk and p38 in mice. Food Chem. Toxicol. 81: 1–8.

Ma, G.Z., Liu, C.H., Wei, B., Qiao, J., Lu, T., Wei, H.C., Chen, H.D., and He, C.D. (2013). Baicalein inhibits DMBA/TPA-induced skin tumorigenesis in mice by modulating proliferation, apoptosis, and inflammation. Inflammation 36(2): 457–467.

Müller-Decker, K., Neufang, G., Berger, I., Neumann, M., Marks, F., and Furstenberger, G. (2002). Transgenic cyclooxygenase-2 overexpression sensitizes mouse skin for carcinogenesis. Proc. Natl. Acad. Sci. USA 99(19): 12483–12488.

Nelson, M.A., Futscher, B.W., Kinsella, T., Wymer, J., and Bowden, G.T. (1992). Detection of mutant Ha-ras genes in chemically initiated mouse skin epidermis before the development of benign tumors. Proc. Natl. Acad. Sci. USA 89(14): 6398–6402.

Pan, M.H., and Ho, C.T. (2008). Chemopreventive effects of natural dietary compounds on cancer development. Chem. Soc. Rev. 37(11): 2558–2574.

Passos, G.F., Medeiros, R., Marcon, R., Nascimento, A.F., Calixto, J.B., and Pianowski, L.F. (2013). The role of PKC/ERK1/2 signaling in the anti-inflammatory effect of tetracyclic triterpene euphol on TPA-induced skin inflammation in mice. Eur. J. Pharmacol. 698(1-3): 413–420.

Qian, K., Wang, G., Cao, R., Liu, T., Qian, G., Guan, X., Guo, Z., Xiao, Y., and Wang, X. (2016). Capsaicin Suppresses Cell Proliferation, Induces Cell Cycle Arrest and ROS Production in Bladder Cancer Cells through FOXO3a-Mediated Pathways. Molecules 21(10): 1406.

Qiu, J., Shi, Z., and Jiang, J. (2017). Cyclooxygenase-2 in glioblastoma multiforme. Drug discovery today 22(1): 148–156.

Rice, N.R., and Ernst, M.K. (1993). In vivo control of NF-kappa B activation by I kappa B alpha. EMBO J. 12(12): 4685–4695.

Ryu, J.H., Park, H.J., Jeong, Y.Y., Han, S., Shin, J.H., Lee, S.J., Kang, M.J., Sung, N.J., and Kang, D. (2015). Aged red garlic extract suppresses nitric oxide production in lipopolysaccharide-treated RAW 264.7 macrophages through inhibition of NF-kappa B. J. Med. Food 18(4): 439–445.

Sahbaz, A., Isik, H., Aynioglu, O., Gungorduk, K., and Gun, B.D. (2014). Effect of intraabdominal administration of Allium sativum (garlic) oil on postoperative peritoneal adhesion. Eur. J. Obstet. Gynecol. Reprod. Biol. 177: 44–47.

Sarkar, F.H., Adsule, S., Li, Y., and Padhye, S. (2007). Back to the future:

COX-2 inhibitors for chemoprevention and cancer therapy. Mini-Rev. Med. Chem. 7(6): 599–608.
Seibert, K., and Masferrer, J.L. (1994). Role of inducible cyclooxygenase (COX-2) in inflammation. Receptor 4(1): 17–23.
Sharma, S.K., Vij, A.S., and Sharma, M. (2013). Mechanisms and clinical uses of capsaicin. Eur. J. Pharmacol. 720(1-3): 55–62.
Shen, C., Wang, S., Shan, Y., Liu, Z., Fan, F., Tao, L., Liu, Y., Zhou, L., Pei, C., Wu, H., Tian, C., Ruan, J., Chen, W., Wang, A., Zheng, S., and Lu, Y. (2014). Chemomodulatory efficacy of lycopene on antioxidant enzymes and carcinogen-induced cutaneum carcinoma in mice. Food Funct. 5(7): 1422–1431.
Shin, J.H., Ryu, J.H., Kang, M.J., Hwang, C.R., Han, J., and Kang, D. (2013). Short-term heating reduces the anti-inflammatory effects of fresh raw garlic extracts on the LPS-induced production of NO and pro-inflammatory cytokines by downregulating allicin activity in RAW 264.7 macrophages. Food Chem. Toxicol. 58: 545–551.
Sobolewski, C., Cerella, C., Dicato, M., Ghibelli, L., and Diederich, M. (2010). The role of cyclooxygenase-2 in cell proliferation and cell death in human malignancies. Int. J. Cell Biol. 2010: 215158.
Steinmetz, K.A., and Potter, J.D. (1996). Vegetables, fruit, and cancer prevention: a review. J. Am. Diet Assoc. 96(10): 1027–1039.
Wang, D., and Dubois, R.N. (2006). Prostaglandins and cancer. Gut 55(1): 115–122.
Wang, M.T., Honn, K.V., and Nie, D. (2007). Cyclooxygenases, prostanoids, and tumor progression. Cancer Metastasis Rev. 26(3-4): 525–534.
Wu, J.C., Wang, F.Z., Tsai, M.L., Lo, C.Y., Badmaev, V., Ho, C.T., Wang, Y.J., and Pan, M.H. (2015). Se-Allylselenocysteine induces autophagy by modulating the AMPK/mTOR signaling pathway and epigenetic regulation of PCDH17 in human colorectal adenocarcinoma cells. Mol. Nutr. Food Res. 59(12): 2511–2522.
Xie, Q.W., Kashiwabara, Y., and Nathan, C. (1994). Role of transcription factor NF-kappa B/Rel in induction of nitric oxide synthase. J. Biol. Chem. 269(7): 4705–4708.
Yamamizu, K., Hamada, Y., and Narita, M. (2015). kappa Opioid receptor ligands regulate angiogenesis in development and in tumours. Br. J. Pharmacol. 172(2): 268–276.
Zhu, Z., Jiang, W., Ganther, H.E., Ip, C., and Thompson, H.J. (2000a). Activity of Se-allylselenocysteine in the presence of methionine gamma-lyase on cell growth, DNA integrity, apoptosis, and cell-cycle regulatory molecules. Mol. Carcinog. 29(4): 191–197.
Zhu, Z., Jiang, W., Ganther, H.E., Ip, C., and Thompson, H.J. (2000b). In vitro effects of Se-allylselenocysteine and Se-propylselenocysteine on cell growth, DNA integrity, and apoptosis. Biochem. Pharmacol. 60(10): 1467–1473.